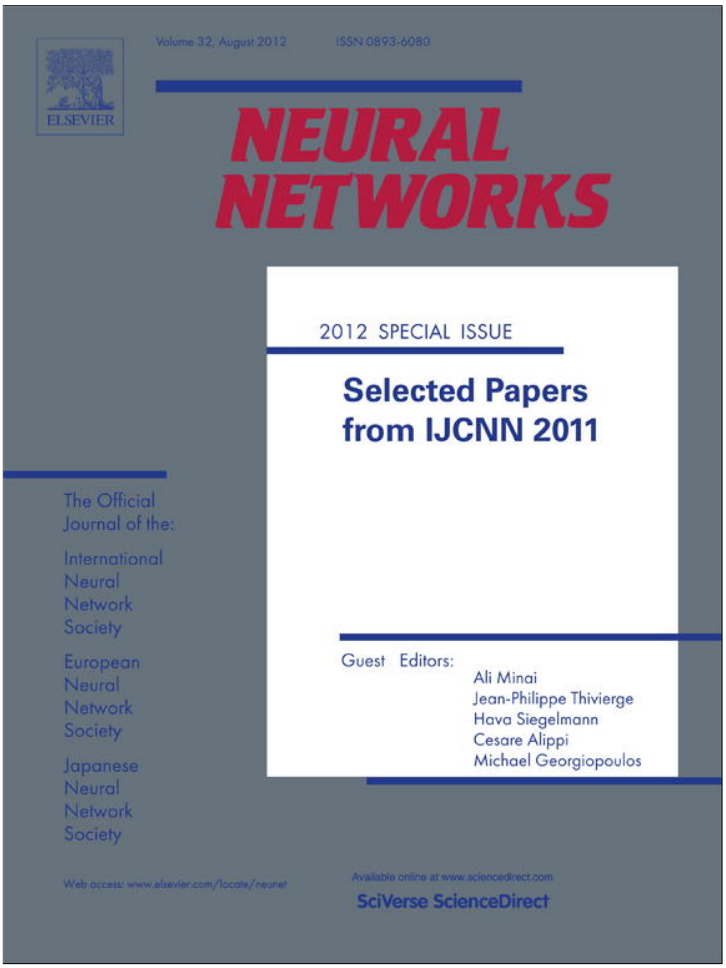

Neural Networks 32 (2012) 313–322

Contents lists available at SciVerse ScienceDirect

Neural Networks

journal homepage: www.elsevier.com/locate/neunet

2012 Special Issue

Identification of brain regions responsible for Alzheimer's disease using a Self-adaptive Resource Allocation Network

B.S. Mahanand [a], S. Suresh [b,*], N. Sundararajan [a], M. Aswatha Kumar [c]

[a] Department of Information Science and Engineering, Sri Jayachamarajendra College of Engineering, Mysore, India
[b] School of Computer Engineering, Nanyang Technological University, Singapore
[c] Department of Information Science and Engineering, M S Ramaiah Institute of Technology, Bangalore, India

ARTICLE INFO

Keywords:
Alzheimer's disease
Magnetic Resonance Imaging
Voxel-based morphometry
Self-adaptive Resource Allocation Network
Integer coded genetic algorithm

ABSTRACT

In this paper, we present a novel approach for the identification of brain regions responsible for Alzheimer's disease using the Magnetic Resonance (MR) images. The approach incorporates the recently developed Self-adaptive Resource Allocation Network (SRAN) for Alzheimer's disease classification using voxel-based morphometric features of MR images. SRAN classifier uses a sequential learning algorithm, employing self-adaptive thresholds to select the appropriate training samples and discard redundant samples to prevent over-training. These selected training samples are then used to evolve the network architecture efficiently. Since, the number of features extracted from the MR images is large, a feature selection scheme (to reduce the number of features needed) using an Integer-Coded Genetic Algorithm (ICGA) in conjunction with the SRAN classifier (referred to here as the ICGA–SRAN classifier) have been developed. In this study, different healthy/Alzheimer's disease patient's MR images from the Open Access Series of Imaging Studies data set have been used for the performance evaluation of the proposed ICGA–SRAN classifier. We have also compared the results of the ICGA–SRAN classifier with the well-known Support Vector Machine (SVM) and Extreme Learning Machine (ELM) classifiers. The study results clearly show that the ICGA–SRAN classifier produces a better generalization performance with a smaller number of features, lower misclassification rate and a compact network. The ICGA–SRAN selected features clearly indicate that the variations in the gray matter volume in the parahippocampal gyrus and amygdala brain regions may be good indicators of the onset of Alzheimer's disease in normal persons.

1. Introduction

Alzheimer's Disease (AD), is considered as one of the most common causes of dementia. AD is a progressive, neuro-degenerative disorder that leads to memory loss, problems in learning, confusion and poor judgment. The only way of diagnosing AD definitively is by doing a post-mortem examination of the brain. During a brain autopsy, AD is diagnosed by identifying the neurofibrillary tangles and amyloid plaque deformities in the brain (Thompson et al., 2007). Early detection of AD using non-invasive methods play a major role in providing treatment that may slow down its progress. One such non-invasive method of early detection of AD is by brain imaging. Commonly used brain imaging techniques for this purpose are Computed Tomography (CT) (Jobst, Barnetson, & Shepstone, 1998; Lopez et al., 1995), Single-Photon Emission Computed Tomography (SPECT), Positron Emission Tomography (PET) (López et al., 2011; Ramírez et al., 2009) and Magnetic Resonance Imaging (MRI) (Davatzikos, Fan, Wu, Shen, & Resnick, 2008; Klöppel et al., 2008).

Studies using CT scans for AD diagnosis have been described in Lopez et al. (1995) and Jobst et al. (1998). However, due to a lower spatial resolution and the possibility of an unreliable structural change detection in the early stages of the disease, CT has been employed only in very few cases. SPECT and PET are functional brain imaging techniques which use a radioactive substance to detect the changes in the blood flow and metabolism in the brain. For AD diagnosis, several studies using SPECT and PET images have been reported in Ramírez et al. (2009) and López et al. (2011). Both PET and SPECT involve the use of ionizing radiation and they are harmful if these are used repeatedly for the study. Hence, the use of PET and SPECT in normal persons is typically limited to a single scan which may not provide adequate information for a proper diagnosis. Also, lack of spatial resolution in the SPECT images influence the accuracy in the detection of AD.

MRI is one of the most important brain imaging procedure that provides an accurate information about the shape and volume of

* Correspondence to: No. 02b-67, Block N4, School of Computer Engineering, Nanyang Technological University, 50 Nanyang Avenue, Singapore 639798, Singapore. Tel.: +65 6790 6185; fax: +65 6792 6559.
E-mail address: ssundaram@ntu.edu.sg (S. Suresh).

0893-6080/$ – see front matter © 2012 Elsevier Ltd. All rights reserved.
doi:10.1016/j.neunet.2012.02.035

the brain. Compared to CT, SPECT and PET scans, MRI provides a high spatial resolution and can detect minute abnormalities in the brain. Usage of MRI for the accurate detection of AD has recently become very active (Davatzikos et al., 2008; Thompson et al., 2007). The problem of early detection of AD from MRI can be cast as a binary classification problem and one can employ machine learning techniques to automatically detect the AD (Chupin et al., 2009; Davatzikos et al., 2008; Klöppel et al., 2008).

The main idea behind using machine learning techniques is to relate the brain volume changes to the onset of AD. Two major ways of estimating the brain volume changes and extracting the necessary features from the MRI are: Regions-of-Interest (ROI) and whole brain morphometric approaches. In the ROI approaches, the volumetric measurements of specific brain regions are used to detect AD. Studies have shown that the tissue loss of the hippocampus and the entorhinal cortex could be indicators for early AD (Jack et al., 1999; Killiany et al., 2002). In Frisoni et al. (1999), the volumes of manually segmented hippocampus and entorhinal cortex is measured to discriminate between the AD patients and normal persons. Major shortcomings in the use of the manual ROI approach are: it is dependent on the tracer's expertise, is time-consuming and error-prone. Recently, an automatic method for the segmentation of the hippocampus using probabilistic and anatomical priors have been proposed for the detection of AD patients (Chupin et al., 2009). In Chupin et al. (2009), automatically segmented hippocampus volumes have been used to classify AD patients and normal persons. Although, ROI techniques for AD analysis have been widely used, they are difficult to accurately identify the brain volume changes in the AD patients when the tissue loss is generally smaller. To overcome these shortcomings, whole brain morphometric approaches have been employed for an accurate AD diagnosis.

Brain morphometry is concerned with the quantification of tissue volume changes in individual brains or between the brains of normal and abnormal persons. MRI based brain morphometric approaches have been used to accurately characterize the brain structure and extract the morphometric features. In these approaches, the features are represented as the probabilities of the gray matter, white matter and cerebrospinal fluid tissue classes in a given voxel, where a voxel is defined as a volume element representing the intensity of a point in a three-dimensional space (Ashburner & Friston, 2000).

In the literature, AD classification studies have been conducted using morphometric features and Support Vector Machine (SVM) classifier (Davatzikos et al., 2008; Klöppel et al., 2008). These methods use different morphological features and different data sets for AD detection. In Klöppel et al. (2008), 90 samples (33 probable mild AD patients and 57 normal) from Rochester, Minnesota was used. A statistical parametric map on gray matter tissues was obtained using these 90 samples and this map was used to extract the features for a SVM classifier. In Davatzikos et al. (2008), a mass-preserving Regional Analysis of Volumes Examined in Normalized Space (RAVENS) was used to extract the features from a smaller set of Baltimore longitudinal study data. Here, 15 probable mild AD patients and 15 normal person's samples are used for the AD detection. RAVENS based feature extraction and SVM classifier provide good performance, but the feature extraction process is computationally intensive. For completely mild AD patients data, the computational effort in RAVENS increases further and it influence the accuracy of the features extracted which affects the SVM classifier performance. Although, AD detection using a SVM classifier has been widely reported (Davatzikos et al., 2008; Klöppel et al., 2008), it requires a significant computational effort for the training process and has a slower training speed.

In this paper, we present a fast and fully automated Voxel-based Morphometry (VBM) approach to identify the regional gray matter differences between the brains of normal persons and AD patients (Ashburner & Friston, 2000). VBM approach uses a unified segmentation and smoothing process to obtain efficient gray matter images from the MRI scans. A statistical analysis is then carried out to extract the volumetric changes in the brain using these gray matter images obtained from both the AD patients and normal persons. VBM approach is efficient due to its unified segmentation process and computationally less intensive due to the use of a linear model for the statistical analysis (Ashburner & Friston, 2005). The unified segmentation method combines the tissue segmentation process, image registration process and bias correction process in a single generative model. The structural MR images are segmented into gray matter, white matter, cerebrospinal fluid and non-brain tissue classes. Compared to the earlier sequential preprocessing methods used in the VBM approach, the current VBM approach based on the unified segmentation model is found to be more accurate (Ashburner & Friston, 2005). The segmented and normalized gray matter images are then smoothed by convolving them with a 10 mm full-width at half-maximum isotropic Gaussian kernel. Finally, a statistical analysis using a general linear model is performed on the smoothed gray matter images of normal persons and the AD patients. From this unified VBM approach, significant areas with an increase in gray matter density in the normal persons relative to the AD patients are obtained. VBM detected voxel locations of these significant gray matter areas are used to extract the features which are then used for AD classification purposes.

Recently in Mahanand, Suresh, Sundararajan, and Aswatha Kumar (2011), high dimensional features extracted using VBM have been reduced using the method of principal component analysis and the reduced features have then been used to detect AD using a Self-adaptive Resource Allocation Network (SRAN) (Sateesh Babu & Suresh, 2012; Suresh, Dong, & Kim, 2010) classifier. The basic building block of SRAN classifier is a radial basis function network. SRAN classifier starts with a zero hidden neuron and builds an appropriate number of hidden neurons to approximate the decision surface. SRAN classifier employs a sequential learning algorithm with self-adaptive thresholds to select the appropriate training samples required to approximate the decision function efficiently. For performance evaluation, 30 MR images of normal persons and 30 patients detected with AD have been used from the publicly available Open Access Series of Imaging Studies (OASIS) data set (Marcus et al., 2007). Using the VBM approach, 5788 morphometric features have been extracted from all the 60 MRI volumes and have been reduced using the method of principal component analysis for classification using a SRAN classifier. The results reported in Mahanand et al. (2011) clearly indicate that a set of reduced number of features is sufficient to accurately detect AD.

Since, the number of features are higher than the number of samples, principal component analysis based features may not be accurate. Also, the reduced features do not provide any information on the original voxel's and hence the regions in the brain responsible for AD. Therefore, in this paper we employ an Integer-Coded Genetic Algorithm (ICGA) to select the appropriate (lower number of) voxel's and use a SRAN classifier to detect the AD. We refer to this as the ICGA–SRAN classifier. For performance evaluation, ICGA–SRAN classifier is used to select the best 10, 20, 30 and 45 voxel's out of the set of 5788 features. Using these GA selected lower number of voxel's, we have conducted a 10-fold validation scheme to study the significance of the selected features. The performance of the proposed ICGA–SRAN classifier is then compared with the standard SVM classifier and the Extreme Learning Machine (ELM) (Huang, Chen, & Siew, 2006; Suresh, Saraswathi, & Sundararajan, 2010) classifier using the lower number of features selected by the ICGA–SRAN classifier. The results clearly highlight the advantages of the SRAN classifier. We

have also conducted a neurological significance study by projecting the best voxel's selected using the ICGA–SRAN classifier onto the three-dimensional brain (volume). The results highlight that loss of gray matter in parahippocampal gyrus and amygdala regions may be responsible for Alzheimer's disease, confirming the earlier results from medical research studies presented in Van Hoesen, Augustinack, Dierking, Redman, and Thangavel (2000), Chow and Cummings (2000).

The paper is organized as follows: Section 2 describes the AD detection problem using all the features extracted from MRI with the VBM approach and classifiers based on SRAN, ELM and SVM. Section 3 describes the feature selection scheme using the ICGA and classification based on SRAN classifier. Section 4 summarizes the conclusions from this study.

2. Alzheimer's disease detection using MRI—problem definition

The problem of AD detection using MRI scans consists of two parts. The first part involves a feature extraction scheme using the voxel-based morphometry approach on the MRI scans. In the second part, based on the features obtained from the first part, AD detection is done using a self-adaptive resource allocation network classifier. Accordingly, this section describes both these parts in detail along with a description of the data used in this study first.

2.1. Materials and image acquisition

In our study, the Open Access Series of Imaging Studies (OASIS) data set available in the public domain has been used (Marcus et al., 2007). OASIS data set has a cross-sectional collection of 416 persons covering the adult life-span viz., ages between 18 to 96 including individuals with Alzheimer's disease in an early-stage. The data includes 218 persons aged between 18 to 59 years and 198 persons aged between 60 to 96 years. Of the 198 older persons, 98 had no AD i.e with Clinical Dementia Rating (CDR) of 0, 70 persons were diagnosed with a very mild AD (CDR $= 0.5$), 28 persons were diagnosed with mild AD (CDR $= 1$) and 2 persons with moderate AD (CDR $= 2$). In our study, we have not considered the 70 *very mild* AD patients and have concentrated only on 30 *mild and moderate* AD patients. For normal persons we have used 30 (out of 98) persons to maintain a sample balance in performing the group analysis using VBM.

Whole-brain T1-weighted 3-dimensional MPRAGE (Magnetization-Prepared Rapid-Acquisition Gradient Echo) data sets were acquired using a Siemens 1.5-T vision scanner in a single imaging session. The acquired volumes had 128 sagittal 1.25 mm slices without gaps and pixel resolution of 256×256 (1×1 mm). The demographic details of the persons selected for this study are given in Table 1.

Table 1
Demographic information of persons used in our study.

	AD	Normal
No. of persons	30	30
Sex (F/M)	20/10	22/08
Age (mean, range)	78.03 (65–96)	75.33 (61–90)
CDR (1/2)	28/2	0

2.2. Feature extraction using a voxel-based morphometric approach

Voxel-based Morphometry (VBM) is a voxel-wise comparison of local tissue volumes of gray matter within a group or across groups of persons using MRI scans. In our study, VBM is used to detect significant gray matter differences between the AD patients and normal persons. The VBM detected voxel locations of significant regions were further used as masks in order to extract the features from all gray matter segmented MRI scans. VBM was performed on the OASIS data set consisting of the MR brain images of 30 AD patients and 30 normal persons using the Statistical Parametric Map (SPM) software package (Schaffer, 2011).

In a VBM approach, the brain MR images undergo various preprocessing steps before the voxel-wise parametric tests are carried out on them. In our study, VBM approach based on a recently proposed unified segmentation model is performed (Ashburner & Friston, 2005). The steps involved in our VBM approach are: unified segmentation, smoothing and statistical testing, in that order. The unified segmentation step is a generative modeling approach, in which tissue segmentation, bias correction and image registration are combined in a single model (Ashburner & Friston, 2005). The unified segmentation framework combines deformable tissue probability maps with a Gaussian mixture model. The MR brain images of both the AD patients and normal persons are segmented into gray matter tissue class. The segmented and normalized gray matter images are then smoothed by convolving them with an isotropic Gaussian kernel. In our approach, a 10 mm full-width at half-maximum Gaussian kernel was employed.

For better understanding of the VBM approach, we have shown three planar views (sagittal, coronal and axial) of the original images and images after every stage in the VBM approach in Fig. 1(a–c). Fig. 1(a) shows the different planar views of the MRI scan. From the MRI scan, one has to perform a bias correction, tissue segmentation and register the segmented image in a standard template for removing non-uniform artifacts. The images after undergoing these steps are shown in Fig. 1(b). From this figure, we can see that the unified segmentation in the VBM approach efficiently identifies the gray matter from the MRI scans. These segmented images are now smoothed by convolving them with an isotropic Gaussian kernel and the resultant images are shown in Fig. 1(c). The smoothing process averages the concentration of the gray matter around the voxel and this helps considerably in the subsequent voxel-by-voxel statistical analysis (Ashburner & Friston, 2005).

The smoothed brain volumes of AD patients and normal persons are used in the statistical analysis to identify regions of gray matter concentration that are significantly related to the Alzheimer's disease. These regions will be used to extract the features for accurate identification of Alzheimer's disease. For the statistical analysis, a general linear model is used to detect the volumetric changes in gray matter across the AD patients and normal persons. In our statistical analysis, estimated total intracranial volume is used as a covariate in the design matrix of the general linear model. Also a two-sample t-test is performed on the smoothed images of normal persons and AD patients and a multiple comparison correction method, namely, a family wise error with $P < 0.05$ has been applied. Following the application of the general linear model and statistical tests, the significance of any differences in gray matter volume is ascertained using the theory of Gaussian random fields (Friston et al., 1994). These tests results in a maximum intensity projection map, which will be then used to extract the features from individual segmented gray images for further analysis. For better understanding, we show the maximum intensity projections of the significant voxels in sagittal, coronal and axial views in Fig. 2.

From Fig. 2, it can be noted that there are significant areas with increased gray matter density in the normal persons relative to the AD patients indicating that for the AD patients gray matter in these locations are lower. A total of 5788 features were extracted from the above VBM approach and these features are then used for classification of AD patients. It is found in the literature that the VBM produces different significant areas with increased gray

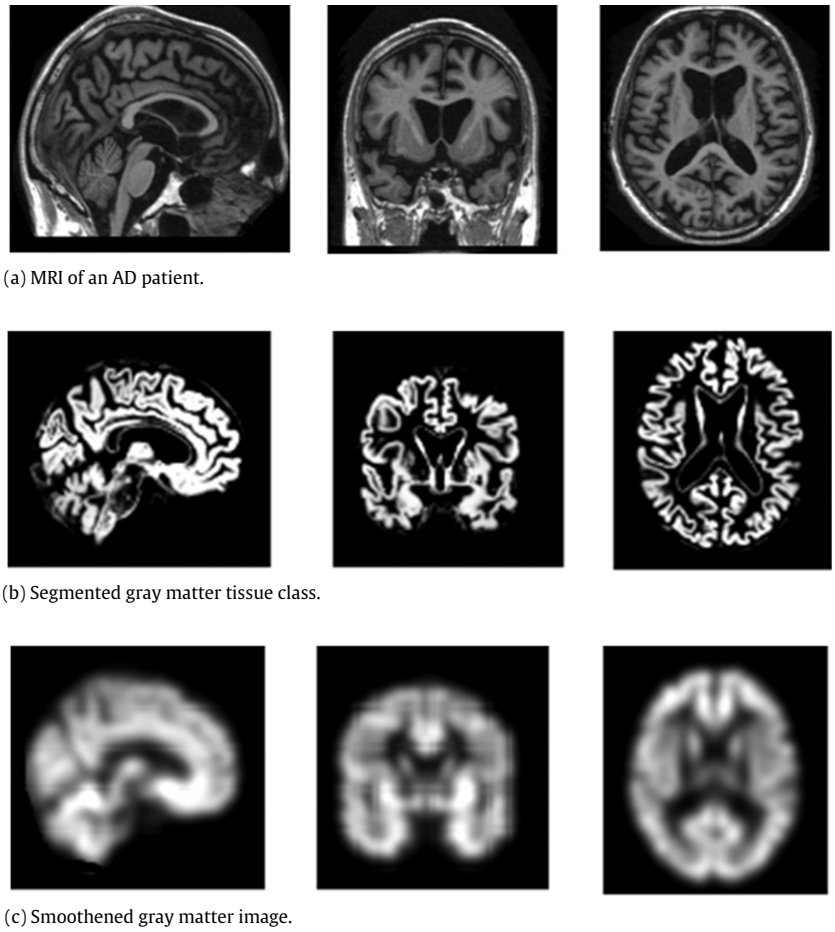

(a) MRI of an AD patient.

(b) Segmented gray matter tissue class.

(c) Smoothened gray matter image.

Fig. 1. Results of the unified segmentation and smoothing steps performed on MRI of an AD patient (from right: sagittal view, coronal view and axial view).

matter density in the brain, when the voxel-wise statistics with different groups of persons (eg. male Vs female, only female etc.) and different covariates (eg. gender, age etc.) are used (García-Sebastián, Savio, Graña, & Villanúa, 2009; Klöppel et al., 2008). This also implies that by employing the above VBM approach one can obtain different sets (with varying numbers) of feature vectors.

To locate the above regions with respect to the spatial locations in the brain, these regions were overlaid on the sliced sections of the commonly used Montreal Neurological Institute (MNI) brain template and the results of the same are shown in Fig. 3. Also, a three-dimensional volume-rendered displays of those significant areas with increased gray matter density in the normal persons relative to the AD patients is shown in Fig. 4. From Figs. 3 and 4, one can infer the regions of the brain which get affected significantly for the AD patients. Putting it differently, during the MRI scans if we can notice that the gray matter in these specific locations are lower, one can infer a good likelihood of developing AD later in these patients.

2.3. Alzheimer's disease detection using the SRAN classifier

In most medical imaging applications, complete set of training data may not be available a priori. Hence, for medical image classification problems, batch learning algorithm may not be suitable and instead on-line/sequential learning algorithms can be used. In on-line/sequential learning, the training samples arrives one-by-one and the samples are deleted after learning. The widely used sequential learning algorithms are: resource allocation network (Platt, 1991), minimal resource allocation network (Yingwei, Sundararajan, & Saratchandran, 1997), growing and pruning RBF network (Huang, Saratchandran, & Sundararajan, 2004) and the sequential multi-category classifier using radial basis function networks (Suresh, Sundararajan, & Saratchandran, 2008b). These sequential algorithms have limitations such as; poor generalization due to over-fitting when more number of similar training data are present, severe class imbalance (Suresh, Sundararajan, & Saratchandran, 2008a) and also the problem dependent algorithm normal person's parameters influence the classification ability of the network. In order to overcome these limitations, recently, a sequential learning algorithm called Self-adaptive Resource Allocation Network (SRAN) has been developed (Suresh, Dong et al., 2010). SRAN classifier uses a radial basis function network as the basic building block along with a set of self-regulated control parameters. SRAN avoids over-training, reduces the learning time, and minimizes the computational effort. Since, it is difficult to get the complete set of AD MRI data a priori, in our work we use a computationally less intensive SRAN classifier for AD detection.

In this section, we present a brief overview of the self-adaptive resource allocation (SRAN) classifier (Suresh, Dong et al., 2010) and how it is used for the Alzheimer's disease detection. Here, we formulate the problem of Alzheimer's disease detection as a binary classification problem deciding whether the person is suffering from AD or not. The 5788 ($n = 5788$) input features ($\mathbf{x}^i$) extracted from ith MRI scans by using the VBM approach is used as an input to the SRAN classifier.

In this study, we have 60 ($N = 60$) observation samples $\{\mathbf{x}^i, y_i\}$, where $\mathbf{x}^i = \left[x_1^i, \ldots, x_n^i\right]^T \in \Re^n$ is a 5788-dimensional feature vector extracted from the ith MRI scan and $y_i \in [1, -1]$ is the coded class label. If the sample belongs to that of an AD patient then the

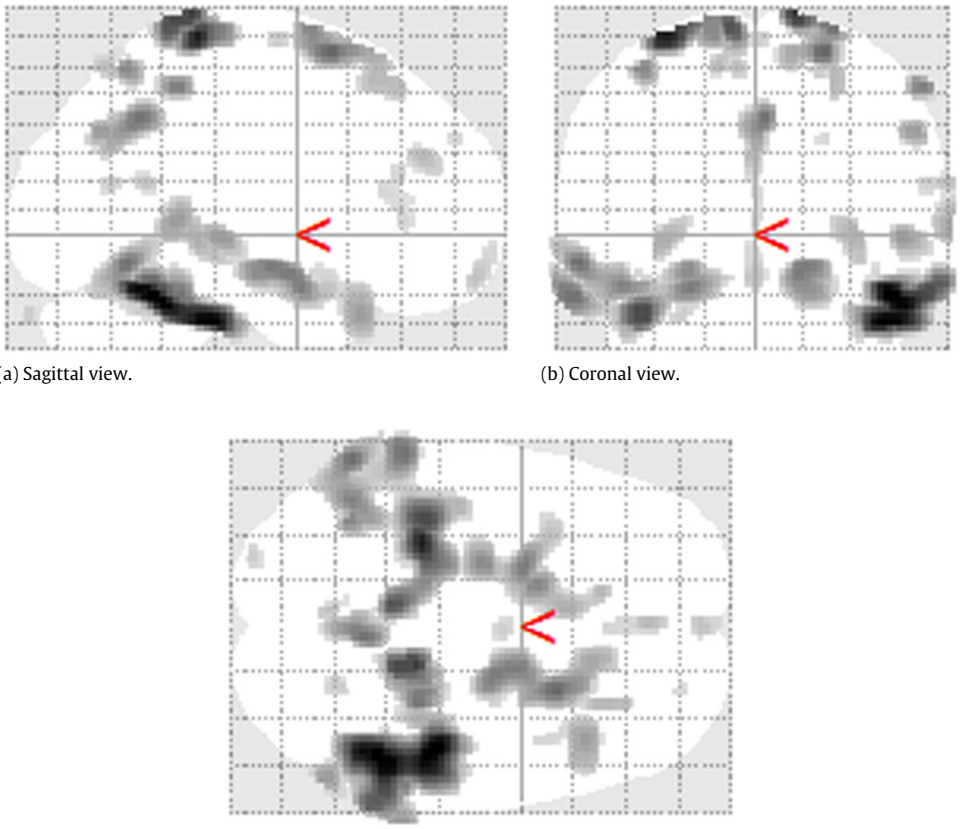

(a) Sagittal view. (b) Coronal view.

(c) Axial view.

Fig. 2. Maximum intensity projections of the significant areas with increased gray matter density in the normal persons relative to the AD patients.

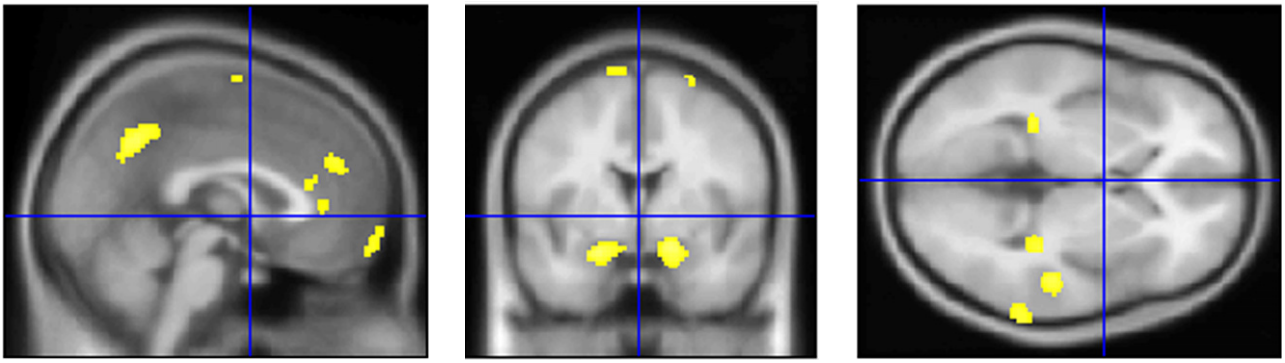

(a) Sagittal view. (b) Coronal view. (c) Axial view.

Fig. 3. Significant areas with increased gray matter density in the normal persons relative to the AD patients overlaid on the MNI template.

coded class label y_i is defined as one ($y_i = 1$), otherwise, sample belongs to normal person where the coded class label is ($y_i = -1$). A classifier function is that function which gives the useful information on the probability of predicting the class label with a desired efficiency and is defined by $Y = F(\mathbf{x})$. For a given a set of samples, the objective of the classification problem is to estimate the functional relationship ($F(.)$) between the random samples and their class labels. In this paper, we employ the SRAN framework to approximate the above functional relationship ($F(.)$).

SRAN classifier is a recently proposed sequential learning algorithm with a self-regulated control mechanism built in it (Suresh, Dong et al., 2010). The SRAN classifier uses a radial function network as the basic building block. In SRAN, when the training sample arrives one-by-one, it computes first the difference in knowledge acquired by the network and the information present in current sample. If the difference is large, either the sample participates in the learning or the sample is pushed into the data stack for later use. If the difference is small, all these redundant samples are deleted from the training set in order to avoid over-training. Also, based on this difference, the network adapts its control parameters.

Without loss of generality, we assume that SRAN builds a classifier with K hidden neurons from sequence of training samples. The network output for the current input feature ($\mathbf{x}^i$) is

$$\hat{y}_j^i = \alpha_{j0} + \sum_{k=1}^{K} \alpha_{jk}\phi_k(\mathbf{x}^i), \quad j = 1, 2, \ldots, n \tag{1}$$

where $\phi_k(\mathbf{x}^i)$ is the response of the kth hidden neuron to the input $\mathbf{x}^i$ and α_{jk} is the weight connecting the kth hidden neuron to the

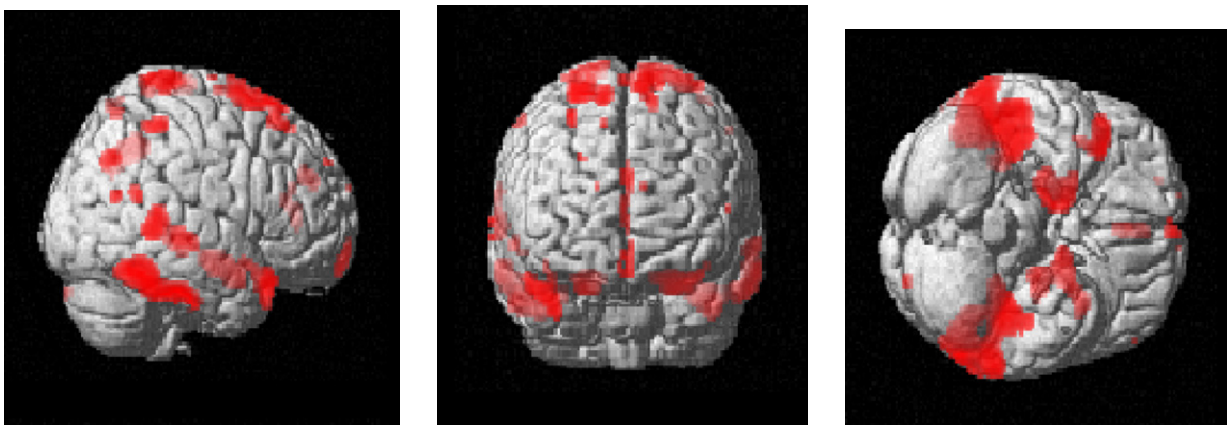

(a) Sagittal view. (b) Coronal view. (c) Axial view.

Fig. 4. Three-dimensional volume-rendered displays of significant areas with increased gray matter density in the normal persons relative to the AD patients.

jth output neuron. The term α_{j0} is the bias term to the jth output neuron.

The response of Gaussian function $\phi_k(\mathbf{x}^i)$ is given by

$$\phi_k(\mathbf{x}^i) = \exp\left(-\frac{\|\mathbf{x}^i - \mu_k^l\|^2}{(\sigma_k^l)^2}\right) \tag{2}$$

where μ_k^l is the center and σ_k^l is the width of the kth hidden neuron which belongs to lth class.

Using the predicted output ($\hat{\mathbf{y}}$), the estimated class label $\hat{c}$ can be obtained as

$$\hat{c} = \arg \max_{i \in 1,2,\ldots,n} \hat{y}_i. \tag{3}$$

The objective of the classifier is to minimize the error between the predicted output ($\hat{\mathbf{y}}$) and actual output ($\mathbf{y}$). In classification problems, it has been shown that the classifier developed using hinge loss function estimates the posterior probability more accurately than the classifier developed using mean square error function (Suresh et al., 2008a). Hence, in SRAN, we use hinge loss error ($\mathbf{e} = [e_1, \ldots, e_N]^T$) and is defined

$$e_j = \begin{cases} 0 & \text{if } \hat{y}_j y_j > 1 \\ \hat{y}_j - y_j & \text{otherwise} \end{cases} \quad j = 1, 2, \ldots, n. \tag{4}$$

The maximum absolute hinge error (E) is given by

$$E = \max_{j=1,\ldots,n} |e_j|. \tag{5}$$

The confidence level of classification or predicted posterior probability is given as

$$\hat{p}(i|\mathbf{x}) = \frac{\min(1, \max(-1, \hat{y}_i)) + 1}{2}, \quad i = 1, 2, \ldots, n. \tag{6}$$

In the setting of standard online/sequential learning, the training sample arrives one at a time and the network adapts its parameters based on the difference in knowledge between the network and the current sample. As each new sample ($\mathbf{x}^i$) is presented to the network, based on the sample error ($\mathbf{e}$), the sample is either

- used for network training (growing/learning) immediately, or
- pushed to the rear end of the stack for learning in future, or
- deleted from the data set.

In ideal conditions, training stops when there are no more samples to be presented to the network. However, in real-time, training is stopped when the samples get stacked repeatedly and do not participate in learning. For complete details on the self-regulatory system of SRAN, one can refer to Suresh, Dong et al. (2010). In our study, the SRAN classifier is used for AD detection since the complete set of AD MRI training data may not be available a priori. Finally, the realized SRAN classifier is compact, avoids over-training, reduces learning time, minimizes the computational effort and provides better generalization performance.

Next, we evaluate the performance of the SRAN classifier and compare the results with a standard SVM classifier and ELM classifier (Huang et al., 2006).

2.4. Performance comparison using all the 5788 features

In our classification study, for each trial, 75% and 25% samples are randomly chosen for training and testing respectively. All the implementations and simulations for SRAN, ELM and SVM classifiers are carried out in a MATLAB 7.9 environment running in an Intel Xeon, 2.33 GHz processor. The SVM experiments are carried out using the libSVM software package (Chang & Lin, 2011). The input features are normalized in the range of $[-1, +1]$ to avoid the dominance of some of the features. For SVM classifier, the cost parameter (c) and kernel width (γ) are selected using a grid search method. The VBM detected morphometric features are used as an input to the classifier. Performance of different classifiers are studied using 20 different random combinations of training and testing data sets to obtain a meaningful mean and standard deviation of the training and testing efficiencies. The mean, standard deviation (STD), the best training/testing efficiencies and training time in seconds for SRAN, ELM and SVM classifiers are presented in Table 2.

From the Table 2, we can see that both SRAN and ELM classifiers produces better testing performance with a lower number of hidden neurons whereas the SVM requires twice the number of hidden neurons as support vectors to produce an average testing efficiency of 89%. The results clearly indicate that SRAN/ELM classifier with all the features produces a 5% improvement in the generalization performance with a fewer number of hidden neurons. SRAN classifier performs slightly better than the ELM classifier with the reduced number of neurons. Also, the training time of SRAN classifier is lower compared to that of the SVM classifier and approximately the same as that of the ELM classifier.

In all medical image classification problems, the misclassification rate plays a very important role along with the correct classification rate for evaluating the classifier performance. In our study, the sensitivity and specificity values are also calculated to find the misclassification rate of the classifier. The sensitivity and specificity factors are defined as

$$Sensitivity = \frac{TP}{TP + FN} \qquad Specificity = \frac{TN}{TN + FP} \tag{7}$$

Table 2
Classification performances of different classifiers on complete feature set.

Classifier	No. of Hidden neurons	Training efficiency			Testing efficiency			Training time in s
		Mean	STD	Best	Mean	STD	Best	
SVM	31	100	0	100	89	6.9	100	0.14
ELM	15	98.37	1.01	100	94.63	5.54	100	0.11
SRAN	14	99.11	0.78	100	95.11	4.25	100	0.12

where TP is the number of true positives: number of AD patients correctly classified; TN is the number of true negatives: number of normal persons correctly classified; FP is the number of false positives: number of normal persons classified as AD patients; FN is the number of false negative: number of AD patients classified as normal persons. It should be noted that in medical problems, sensitivity is more important than specificity as it is better to classify a healthy person as having the disease rather than classifying a diseased person as being healthy.

In our study, the SRAN/ELM classifier with all the 5788 morphometric features produced a mean sensitivity of 0.95 and mean specificity of 0.95 whereas, SVM classifier produced a mean sensitivity of 0.90 and mean specificity of 0.89. This clearly indicates that the SRAN/ELM classifier achieves better classification performance along with a reduced misclassification rate.

3. AD detection using the ICGA–SRAN classifier

The 5788 morphometric features extracted from the MRI scans using the VBM approach represent the regions in the whole brain where gray matter volume changes are significant. Also, the results reported in Mahanand et al. (2011) clearly indicate that all 5788 features may not be required for accurate detection of AD. The regions selected by the VBM approach are shown in Fig. 3. In the literature, studies have shown that loss of gray matter volume in the hippocampus and entorhinal cortex regions could be indicators for early AD (Jack et al., 1999; Killiany et al., 2002). From Fig. 3, we can see that volumetric changes can occur even in other brain regions. In order to identify the relevant features for AD detection, we propose below a feature selection and a classification approach called as the Integer Coded Genetic Algorithm—SRAN (ICGA–SRAN) classifier.

3.1. ICGA–SRAN classifier

Conventionally, feature selection methods are two types, namely, filter approach and wrapper approach. Integer Coded Genetic Algorithm (ICGA) for feature selection is well-known approach in the literature. In the filtering approach, selected features are independent of the choice of classification methods and is suitable for problems with large number of samples. In the wrapper approach, feature selection depends on the choice of the classifier and is suitable for all problems. Many approaches have been implemented by integrating genetic algorithm with neural networks for feature selection and classification (Koller & Sahami, 1996; Saraswathi, Suresh, Sundararajan, Zimmermann, & Nilsen-Hamilton, 2011). In this work, we use ICGA–SRAN classifier based wrapper approach for accurate detection of brain region.

The schematic diagram of the ICGA–SRAN classifier is given in Fig. 5. The ICGA selects M features and the SRAN classifier predicts the training/testing efficiency as a fitness measure for these selected features. On completing the evolutionary search process, the ICGA–SRAN classifier identifies the best M features required for maximizing the AD detection performance. A brief description of the ICGA algorithm is given below.

Integer-Coded Genetic Algorithm.

Genetic algorithms are evolutionary based search techniques (Holland, 1975; Michalewicz, 1994) designed based on the adaptive process of natural systems. Genetic algorithms are widely used to solve complex optimization problems where analytical solutions are difficult to obtain. In recent years, many works have been reported for feature selection using both genetic algorithms and neural networks. A complete survey of this area for feature selection is given in Schaffer, Whitley, and Eshelman (1992).

In a feature selection approach, one needs to identify the best subset of features required to approximate the decision function that maximizes the classification performance i.e. select the independent integers representing the feature numbers from a given set of the full features. For a given problem, the components of ICGA consist of choosing proper (a) string representation; (b) selection function; (c) genetic operators; and (d) the fitness function. In this paper, we use the normalized geometric ranking method as the selection function and a partially mapped crossover and random mutation as genetic operators. The detailed description of these functions can be found in Michalewicz (1994), Suresh, Mani, Omkar, and Kim (2006). The description of the other two components (string representation and fitness function) of ICGA are described below.

String representation. Let us assume that the ICGA selects M independent features from the given set. The length of the string/chromosome is M and the elements of the string represent the independent features as given below

$$S = [x_1,\ x_i,\ x_j, \ldots, x_N]_{1\times M}. \tag{8}$$

Note that the selected features belong to the set S and they are independent.

Fitness function. The objective of feature selection is to find the best set of features that maximizes the classification efficiency. The effectiveness of the selected features (S) can be determined by evaluating training/testing efficiencies of the SRAN classifier. The fitness of the selected feature (S) is defined as

$$F_S = \begin{cases} \eta_a & \text{if } \eta_a < 95\% \\ 1 + \eta_v & \text{otherwise} \end{cases} \tag{9}$$

where η_a is the training efficiency and η_v is the testing efficiency.

3.2. ICGA–SRAN classifier performance results

The ICGA–SRAN classifier has been implemented and tested in a MALTLAB 7.9 environment running on an Intel Xeon, 2.33 GHz processor. Convergence of the ICGA depends on the size of the population (N_p), the selection probability (P_s), the crossover probability (P_c) and the mutation probability (P_m). The ICGA parameters used in our study are: the population size is 10, the maximum number of generations is 5, P_s is 0.08; P_c is 0.7; and P_m is 0.5. For proper parameter selection of ICGA parameters, refer to Michalewicz (1994).

The best solution obtained after a given number of generations is used to build the classifiers. The ICGA–SRAN classifier is called on several times for a fixed number of features, i.e., 10, 20, 30 and 45. The performance of the SRAN, ELM and SVM classifiers on these ICGA selected set of features are evaluated

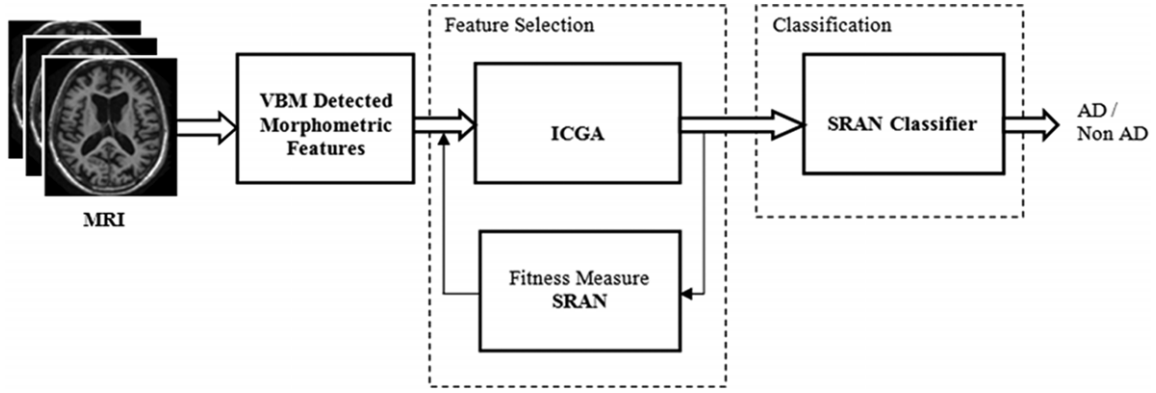

Fig. 5. ICGA–SRAN classifier.

Table 3
Classification performances of different classifiers on ICGA selected feature set.

Selected features	Classifier	No. of Hidden neurons	Training efficiency			Testing efficiency			Training time in s
			Mean	STD	Best	Mean	STD	Best	
10	SVM	18	99.29	1.05	100	86.84	9.15	100	0.06
	ELM	10	98.46	1.05	100	91.86	6.99	100	0.04
	SRAN	14	98.01	2.35	100	92.13	2.71	100	0.04
20	SVM	23	99.76	0.70	100	85.18	10.78	100	0.07
	ELM	14	98.45	1.05	100	88.86	6.55	100	0.05
	SRAN	16	98.26	1.93	100	91.09	4.86	100	0.06
30	SVM	28	98.32	1.00	100	84.15	7.54	100	0.08
	ELM	15	98.34	1.00	100	91.	8.91	100	0.06
	SRAN	16	98.25	1.78	100	89.31	3.62	100	0.07
45	SVM	30	99.65	0.82	100	85.15	8.79	100	0.09
	ELM	15	98.23	0.92	100	90.24	5.99	100	0.07
	SRAN	16	97.12	1.81	100	90.37	5.29	100	0.08

using 20 different random combination of training/testing data. The classification performance of different classifiers using the ICGA selected features is given in Table 3.

From Table 3, it is observed that SRAN produces the mean training efficiency of 98.01% and mean testing efficiency of 92.13% on 10 ICGA selected morphometric features using 14 hidden neurons and 0.04 s of training time. Also, the table indicates that for the case of 10 features, the best training and testing efficiencies are 100% for the 20 random trials. For other combinations of the feature sets, almost similar training and testing efficiencies are obtained using the SRAN classifier. Using the ELM classifier on 10 features, the mean training efficiency of 98.46% and mean testing efficiency of 91.86% are obtained using 10 hidden neurons and 0.04 s of training time. From Table 3, it is also observed that the mean training efficiency of 99.29% and mean testing efficiency of 86.84% are obtained using the SVM classifier with the RBF kernel ($C = 40$, $\gamma = 0.125$) on 10 ICGA selected features using 18 support vectors and 0.05 s of training time. From the experiments using ICGA selected features, we can observe that with only 10 features, SRAN classifier produces the mean testing efficiency higher than that of the ELM and SVM classifiers indicating better generalization with a lower number of features. Also, the training time of SRAN classifier is lower compared to that of the SVM classifier and is around the same value for the ELM classifier.

Fig. 6 shows the sensitivity performance of SRAN, ELM and SVM classifiers on ICGA selected features, where the number of features is the X axis and the sensitivity is along the Y axis.

Fig. 7 shows the specificity performance of SRAN, ELM and SVM classifiers on ICGA selected features, where the number of features is along the X axis and the specificity is along the Y axis.

From Figs. 6 and 7, it is observed that using the SRAN classifier on 10 ICGA selected features the mean sensitivity of 0.97 and mean specificity of 0.88 is obtained. The ELM classifier produces

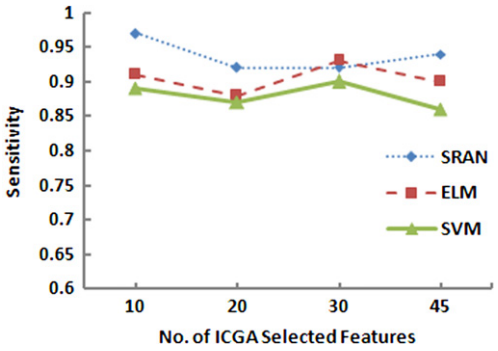

Fig. 6. Sensitivity performance of different classifiers on ICGA selected feature set.

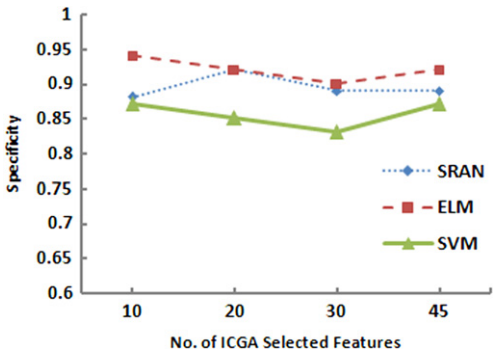

Fig. 7. Specificity performance of different classifiers on ICGA selected feature set.

a mean sensitivity of 0.91 and mean specificity of 0.94 with 10 ICGA selected features. Also, mean sensitivity of 0.89 and mean

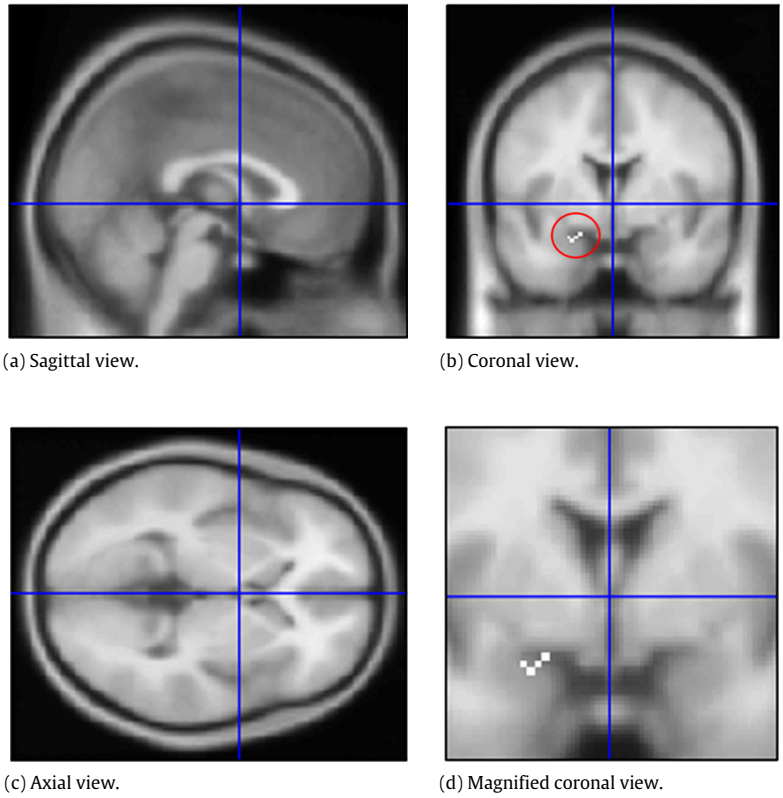

(a) Sagittal view. (b) Coronal view.

(c) Axial view. (d) Magnified coronal view.

Fig. 8. ICGA selected features mapped back into the standard MNI brain space.

specificity of 0.87 is obtained using SVM classifier on the same number of features. Although, the specificity of SRAN classifier is lower than that of the ELM classifier, in AD detection problem, obtaining a better sensitivity is more important than achieving a better specificity. This is because it is always better to err in classifying healthy persons as having AD than to classify AD patients as healthy. This study clearly indicates that the SRAN classifier reduces the misclassification of AD patients to a larger extent and achieves a better classification efficiency with the lower number of features. Hence, it can be inferred from the results obtained that accurate detection of AD from MRI can be performed using SRAN classifier with only 10 ICGA selected morphometric features.

3.3. Neurological significance study

Using the ICGA selected morphometric features, we also conducted a neurological significance study to identify the specific brain regions that are affected in the AD patients. In our study, the 10 ICGA selected features from the 20 trials are mapped back into the standard MNI brain space. The specific brain regions mapped back by the ICGA based feature selection approach are shown in Fig. 8.

From the Fig. 8, it is observed that the 10 ICGA selected features are from the parahippocampal gyrus and amygdala regions of the brain. The parahippocampal gyrus is a gray matter cortical region of the brain which plays an important role in memory encoding and retrieval. The amygdala is an almond-shape set of neurons involved in several brain functions, including emotion, learning and memory. Both the parahippocampal gyrus and amygdala regions are often involved in distinguishing patients with early AD. From the results obtained, it can be inferred that accurate detection of AD can be performed by selecting features only from the parahippocampal gyrus and amygdala regions of the brain. This result confirms similar inferences being highlighted in the medical studies presented in Van Hoesen et al. (2000), Chow and Cummings (2000).

4. Conclusions

This paper presents a new approach for an accurate identification of the brain regions responsible for AD using an ICGA–SRAN classifier for feature selection and classification using voxel based morphometric features from MR images. For performance analysis, OASIS MR images of 30 normal persons and 30 AD patients have been used. Using all the 5788 voxel based morphometric features, the SRAN classifier produced slightly better mean testing efficiency than ELM and SVM classifiers. Hence, SRAN classifier is used in ICGA for selection of different set of features. ICGA–SRAN classifier is used to select 10, 20, 30, 45 features from the complete 5788 features. The study clearly indicates that accurate detection of AD can be performed with only 10 ICGA selected feature using the SRAN classifier. The ICGA–SRAN selected features from the MR images clearly indicate that the critical regions responsible for AD are the parahippocampal gyrus and amygdala regions of the brain. The results from this study indicate that one may look at any variation in gray matter in these brain regions instead of the complete brain volume and this reinforces similar observations based on the pathological analysis of the brain, available in the literature. A problem for future work would be to identify the AD patients prospectively, so that the disease can be detected before the cognitive scores are affected.

Acknowledgments

We thank the Washington University Alzheimer's Disease Research Center for making the MRI data available in the public domain for this study. The authors would like to thank

the reviewers for their valuable suggestions which helped in improving the quality of this paper. The second author acknowledge the support of Academic Research Funding (AcRF) Tier I (No. M58020020) grant.

References

Ashburner, J., & Friston, K. J. (2000). Voxel-based morphometry-the methods. *NeuroImage*, *11*, 805–821.

Ashburner, J., & Friston, K. J. (2005). Unified segmentation. *Neuro Image*, *26*, 839–851.

Chang, C. C., & Lin, C. J. (2011). LIBSVM: a library for support vector machines. *ACM Transactions on Intelligent Systems and Technology*, *2*, 1–27.

Chow, T. W., & Cummings, J. L. (2000). The amygdala and Alzheimers disease. In J. P. Aggleton (Ed.), *The Amygdala: a functional analysis* (pp. 656–680). Oxford: Oxford University Press.

Chupin, M., Gérardin, E., Cuingnet, R., Boutet, C., Lemieux, L., Lehéricy, S., et al. (2009). Fully automatic hippocampus segmentation and classification in Alzheimers disease and mild cognitive impairment applied on data from ADNI. *Hippocampus*, *19*, 579–587.

Davatzikos, C., Fan, Y., Wu, X., Shen, D., & Resnick, S. M. (2008). Detection of prodromal Alzheimer's disease via pattern classification of MRI. *Neurobiology of Aging*, *29*, 514–523.

Frisoni, G. B., Laakso, M. P., Beltramello, A., Geroldi, C., Bianchetti, A., Soininen, H., et al. (1999). Hippocampal and entorhinal cortex atrophy in frontotemporal dementia and Alzheimer's disease. *Neurology*, *52*, 91–100.

Friston, K. J., Holmes, A. P., Worsley, K. J., Poline, J. B., Frith, C. D., & Frackowiak, R. S. J. (1994). Statistical parametric maps in functional imaging: a general linear approach. *Human Brain Mapping*, *2*, 189–210.

García-Sebastián, M., Savio, A., Graña, M., & Villanúa, J. (2009). On the use of morphometry based features for Alzheimer's disease detection on MRI. In *Proceedings of the 10th international work-conference on artificial neural networks: part i: bio-inspired systems: computational and ambient intelligence* (pp. 957–964).

Holland, H. J. (1975). *Adaptation in natural and artificial systems*. Ann Arbor: University of Michigan Press.

Huang, G. B., Chen, L., & Siew, C. K. (2006). Universal approximation using incremental constructive feedforward networks with random hidden nodes. *IEEE Transactions on Neural Networks*, *17*, 879–892.

Huang, G. B., Saratchandran, P., & Sundararajan, N. (2004). An efficient sequential learning algorithm for growing and pruning RBF (GAP-RBF) networks. *IEEE Transactions on Systems, Man, and Cybernetics, Part B: Cybernetics*, *34*, 2284–2292.

Jack, C. R., Jr, Petersen, R. C., Xu, Y. C., O'Brien, P. C., Smith, G. E., Ivnik, R. J., et al. (1999). Prediction of AD with MRI-based hippocampal volume in mild cognitive impairment. *Neurology*, *52*, 1397–1403.

Jobst, K. A., Barnetson, L. P., & Shepstone, B. J. (1998). Accurate prediction of histologically confirmed Alzheimer's disease and the differential diagnosis of dementia: the use of NINCDS-ADRDA and DSM-III-R criteria, SPECT, X-ray CT, and apo E4 in medial temporal lobe dementias. Oxford project to investigate memory and aging. *International Psychogeriatrics*, *10*, 271–302.

Killiany, R. J., Hyman, B. T., Gomez-Isla, T., Moss, M. B., Kikinis, R., Jolesz, F., et al. (2002). MRI measures of entorhinal cortex vs hippocampus in preclinical AD. *Neurology*, *58*, 1188–1196.

Klöppel, S., Stonnington, C. M., Chu, C., Draganski, B., Scahill, R. I., Rohrer, J. D., et al. (2008). Automatic classification of MR scans in Alzheimer's disease. *Brain*, *131*, 681–689.

Koller, D., & Sahami, M. (1996). Toward optimal feature selection. In *Proceedings of international conference on machine learning* (pp. 284–292).

Lopez, O. L., Becker, J. T., Jungreis, C. A., Rezek, D., Estol, C., Boller, F., et al. (1995). Computed tomography – but not magnetic resonance imaging – identified periventricular white-matter lesions predict symptomatic cerebrovascular disease in probable Alzheimer's disease. *Archives of Neurology*, *52*, 659–664.

López, M., Ramírez, J., Górriz, J. M., Álvarez, I., Salas-Gonzalez, D., Segovia, F., et al. (2011). Principal component analysis-based techniques and supervised classification schemes for the early detection of Alzheimer's disease. *Neurocomputing*, *74*, 1260–1271.

Mahanand, B. S., Suresh, S., Sundararajan, N., & Aswatha Kumar, M. (2011). Alzheimers disease detection using a self-adaptive resource allocation network classifier. In *Proceedings of international joint conference on neural networks* (pp. 1930–1934).

Marcus, D. S., Wang, T. H., Parker, J., Csernansky, J. G., Morris, J. C., & Buckner, R. L. (2007). Open access series of imaging studies (OASIS): cross-sectional MRI data in young, middle aged, nondemented, and demented older adults. *Journal of Cognitive Neuroscience*, *19*, 1498–1507.

Michalewicz, Z. (1994). *Genetic algorithms + data structures = evolution programs*. New York: Springer-Verlag.

Platt, J. (1991). A resource-allocating network for function interpolation. *Neural Computation*, *3*, 213–225.

Ramírez, J., Górriz, J. M., López, M., Salas-Gonzalez, D., Álvarez, I., Segovia, F., et al. (2009). Early detection of the Alzheimer's disease combining feature selection and kernel machines. In M. Köppen, N. Kasabov, & G. Coghill (Eds.), *Advances in neuro-information processing: vol. 5507* (pp. 410–417). Berlin, Heidelberg: Springer.

Saraswathi, S., Suresh, S., Sundararajan, N., Zimmermann, M., & Nilsen-Hamilton, M. (2011). ICGA-PSO-ELM approach for accurate multiclass cancer classification resulting in reduced gene sets in which genes encoding secreted proteins are highly represented. *IEEE/ACM Transactions on Computational Biology and Bioinformatics*, *8*, 452–463.

Sateesh Babu, G., & Suresh, S. (2012). Meta-cognitive neural network for classification problems in a sequential learning framework. *Neurocomputing*, *81*, 86–96.

Schaffer, J. D., Whitley, D., & Eshelman, L. J. (1992). Combinations of genetic algorithms and neural networks: a survey of the state of the art. In *Proceedings of international workshop on combinations of genetic algorithms and neural networks* (pp. 1–37).

SPM8 (2011). Wellcome trust center for neuroimaging, Institute of neurology, UCL, London, UK. http://www.fil.ion.ucl.ac.uk/spm/.

Suresh, S., Mani, V., Omkar, S. N., & Kim, H. J. (2006). Divisible load scheduling in tree network with limited memory: a genetic algorithm and linear programming approach. *International Journal of Parallel Emergent and Distributed System*, *21*, 303–321.

Suresh, S., Dong, K., & Kim, H. J. (2010). A sequential learning algorithm for self-adaptive resource allocation network classifier. *Neurocomputing*, *73*, 3012–3019.

Suresh, S., Saraswathi, S., & Sundararajan, N. (2010). Performance enhancement of extreme learning machine for multi-category sparse data classification problems. *Engineering Application of Artificial Intelligence*, *23*, 1149–1157.

Suresh, S., Sundararajan, N., & Saratchandran, P. (2008a). Risk sensitive hinge loss functions for sparse multi-category classification problems. *Information Sciences*, *178*, 2621–2638.

Suresh, S., Sundararajan, N., & Saratchandran, P. (2008b). A sequential multi-category classifier using radial basis function networks. *Neurocomputing*, *71*, 1345–1358.

Thompson, P. M., Hayashi, K. M., Dutton, R. A., Chiang, M. C., Leow, A. D., Sowell, E. R., et al. (2007). Tracking Alzheimers disease. *Annals Of The New York Academy Of Sciences*, *1097*, 183–214.

Van Hoesen, G. W., Augustinack, J. C., Dierking, J., Redman, S. J., & Thangavel, R. (2000). The parahippocampal gyrus in Alzheimer's disease. Clinical and preclinical neuroanatomical correlates. *Annals of the New York Academy of Sciences*, *911*, 254–274.

Yingwei, L., Sundararajan, N., & Saratchandran, P. (1997). A sequental learning scheme for function approximation using minimal radial basis function neural networks. *Neural Computation*, *9*, 461–478.